# Study of the Diffusion of Cu(II) as an Oxidant Through Simulated Particle Pores in a Novel Model Apparatus


**B. Manana, J. Petersen and R. Ram**

**Abstract** In heap leaching, the oxidative dissolution of value minerals encapsulated deep within large particles cannot be fully understood on the basis of the bulk solution conditions relative to variable solution conditions near the mineral surface. In the present study, the diffusion of the oxidising species through inner particle pores is simulated in a model apparatus that separates an inert platinum electrode under controlled reduction potential from the bulk solution through narrow pores of varying length. The Cu-$NH_3$ system was selected as a model system and Cu(II)/Cu(I) as the redox couple of interest. Platinum probes inserted in the pores allowed the measurement of varying redox potentials along the pore length. Results showed that in a 10 mm pore, there exists a narrow (0.5 mm) zone near the reduction surface that is depleted of the oxidant and in which its supply is strongly diffusion limited, even if it is in abundance in the bulk solution. The consistent presence of this narrow diffusion region across all experimental results indicated that the transportation of the reduced species away from the reaction surface had the most significant influence on the potential variations within the pore. This was further supported by the minimal effect of varying concentrations of both Cu(II) and dissolved oxygen on the solution potential within this region.

B. Manana · J. Petersen (✉) · R. Ram
Minerals to Metals Initiative, Department of Chemical Engineering, University of Cape Town, Private Bag X6, Rondebosch 7701, South Africa
e-mail: jochen.petersen@uct.ac.za

B. Manana
e-mail: buhle.manana@gmail.com

R. Ram
e-mail: rahul.ram@monash.edu

B. Manana · J. Petersen · R. Ram
Hydromet Research Group, Department of Chemical Engineering, University of Cape Town, Private Bag X6, Rondebosch 7701, South Africa

R. Ram
School of Earth, Atmosphere and Environment, Monash University, Building 28, 9 Rainforest Walk, Clayton 3800, Australia



B. Davis et al. (eds.), *Extraction 2018*, The Minerals, Metals & Materials Series,
https://doi.org/10.1007/978-3-319-95022-8_111

**Keywords** Heap leaching · Intra-particle diffusion · Electrochemical potential Copper · Ammonia

## Introduction

Heap leaching has become a major contributor to the extraction of metals from low to mixed grade ore resources, particularly copper, gold, uranium and silver [1]. It is most applicable to low grade ores as it requires minimal size reduction to relatively coarse particle sizes, with the particle size distribution typically in the range of 12–25 mm for crushed and agglomerated ore [2]. As coarser particles are used, there is a distribution of value mineral grains within the heap with varying degrees of liberation and accessibility to leaching solution. The leachability of the mineral grain is determined by its accessibility to the solution phase, as experimental evidence has shown that leaching occurs in the interfacial region between the mineral grain surface and the leaching solution [3, 4]. Mineral grains occluded within the particle may be exposed to the leaching solution via cracks or diffusion pore networks induced during the crushing process. Mineral extraction rates have shown an initially fast rate, allowing for 60% extraction in the first few months, and a subsequently slower rate which allows for 80–90% extraction over a period of 12–24 months. This has been attributed to the changeover of leaching from surface exposed grains, to the more inaccessible grains within the particle [5].

Considering the individual ore particle with mineral inclusions, when the diffusion pore is saturated with solution, dissolved reagents may diffuse to the mineral surface where they react, whilst the solution itself remains stagnant. Conversely, the reaction products are transported away from the mineral surface to the bulk solution at the end of the pore [6].

In oxidative leaching of copper sulphides in ammonia, the primary oxidant (Cu (II)) reacts with the mineral surface, and is consequently reduced. The reduced species (Cu(I)) is then transported away from the surface and is homogeneously re-oxidized by a soluble secondary oxidant (dissolved oxygen), as illustrated in Fig. 1. The presence of diffusion pores/cracks in coarse particles, presents a diffusion obstacle for the transportation and re-oxidation of the reduced species (Cu(I)) away from the mineral surface and the replenishment of the oxidant (Cu(II)) at the

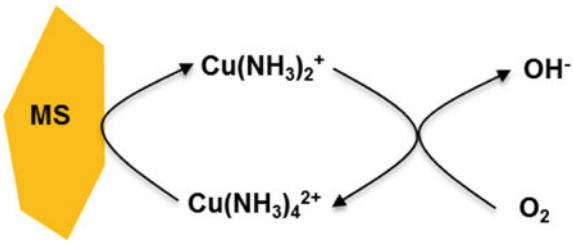


**Fig. 1** Illustration of the reduction-oxidation reactions that occur during the leaching of a mineral sulfide (denoted MS) in ammoniacal solutions and in the presence of oxygen

surface. The hindered mass transport of these species results in concentration gradients within the pore. The potential of the system is related to the activities (estimated as concentrations in dilute solutions) of the oxidised and reduced species present in that solution, through the Nernst equation. In the presence of ammonia, the equilibrium potential was computed by Meng and Han [7] to incorporate complexation with ammonia:

$$E_{eq} = 0.074 - 0.1182 \log[NH_3] + \frac{2.303RT}{nF} \log \frac{[Cu(NH_3)_4^{2+}]}{[Cu(NH_3)_2^{+}]} \quad (1)$$

## Materials and Methods

### *Materials*

Test solutions were prepared using reagent grade $(NH_4)_2SO_4$ and 25% w/w $NH_4OH$ in equal molar ratios, in deionized water to make a 2 M total ammonia solution. Cupric ions (Cu(II)) were introduced to the solutions in varying quantities as required, by dissolving $CuSO_4 \cdot 5H_2O$. For tests that required oxygen or nitrogen, the gases were sparged at flowrate of 1 L/min to the solution with ca. 100 rpm magnetic stirring for a period of 10 min prior to experimentation. Thereafter the flowrate was decreased and maintained at 0.5 L/min on the surface of the solution throughout the experiment, magnetic agitation was halted during the experimental process.

Electrochemical tests were conducted in a 250 mL constant temperature glass reactor with a saturated calomel electrode as the reference electrode and platinum as the counter electrode. A cylindrical platinum electrode (denoted Pt-E), embedded in Teflon, was used as the reaction surface, with a diameter of 5 mm and a reaction surface area of 0.1963 $cm^2$. All electrodes were frequently calibrated in standard redox solution. All electrochemical measurements are quoted with reference to the SHE scale.

### *Methodology*

A system that models a reactive mineral grain surface encapsulated within an inert ore particle with a straight (non-tortuous) crack through the ore was developed following the concept proposed by Nicol and Basson [8].

## Development of Ore Particle Model System

Teflon disks were used to model thin cross sections of an individual cylindrical non-reactive ore particle with pores/cracks through the centre. Circular disks of 30 mm diameter and varying thicknesses (0.25 mm, 1 mm and 2 mm) were constructed from Teflon. With the disks aligned, three perforations of 1 mm diameter were drilled through the centre and four 4 mm diameter holes were drilled around the circumference. A Teflon fitting to bind and secure the disks onto the Pt-E electrode was constructed. Stacking the Teflon disks to a desired length ($l$ mm) resulted in three continuous diffusion pores of 1 mm each at the centre of the disks as shown in Fig. 2.

Upon placing in solution, the solution is allowed to seep through continuous pore spaces in the stacked disks to the Pt-E surface by capillary action. The system modelled a mineral grain at the end of a diffusion pore through a (Pt-E) surface encapsulated in inert gangue (Teflon disks) with three continuous pores leading to the 'particle' surface. With the Teflon disk stack attached to the Pt-E electrode, the effective exposed reaction surface was 0.02356 $cm^2$.

Nylon disks of the same dimension as the Teflon disks were used to hold thin cylindrical platinum wires of 0.1 mm diameter and 5 mm in length to be used for potential measurements. These were connected to one exposed end of insulated stainless steel (SS) wires using conductive silver paste. The wires were then embedded into the nylon disks and a monolayer of epoxy paint was applied to insulate exposed silver paste and SS wires on the surface, leaving only the platinum wires exposed within in the 1 mm holes (Fig. 2). These probes were then calibrated in standard redox solution, prior to inserting at the desired position ($l$ mm) within the Teflon stack. The platinum probes were sufficiently thin so as to not obstruct the cross-section available for diffusion; the wire occupied only about 12% of the cross-sectional area.

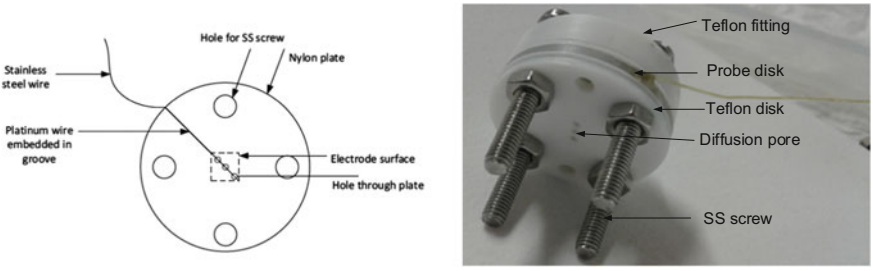


**Fig. 2** Experimental model cell for an encapsulated ore particle

### Electrochemical Analyses

The three electrode system was assembled, with the disk-electrode assembly stacked to the desired diffusion pore length (denoted *l*) containing the nylon-platinum probe at the desired probe position away from the Pt surface is denoted *y* (mm). The three electrode system was connected to a Gamry Series G 300/750 potentiostat which was controlled by Gamry Framework software, and the required electrochemical techniques were applied.

A summary of the sequence of the electrochemical techniques is detailed below:

1. Set up the three electrode system, adjust solution parameters and measure the Open Circuit Potential (OCP) using the Pt-E as the working electrode.
2. Attach the Teflon stack with the probe at the desired position (*y)* and measure the solution potential using the probe, ensuring it is within ± 10 mV of the potential noted in Step 1.
3. Connect the Pt-E as the working electrode and run potentiostatic tests to drive the reduction reaction at the surface. Measure current density for a period of 800 s.
4. Immediately after termination of the cathodic reaction, disconnect the Pt-E electrode and use the probe to conduct OCP measurements.
5. Wait for the system to re-equilibrate to the initial bulk potential from Step 1. Triplicate the procedure for every probe position, before varying the position (*l* mm) of the probe.

OCPs were generated at 25 °C in 2 M unstirred ammonia solution of pH 9.6 ± 0.3 with the reaction vessel open to atmosphere, with oxygen present in air, and was measured to be 283 ± 5 mV (SHE). Cyclic Voltammograms (CV) were generated at a scan rate of 5 mV/s on the stationary Pt-E surface to determine operating conditions. The forward (anodic) sweep limit was set at +395 mV and the backward (cathodic) limit was set at −260 mV. Potentiostatic experiments were conducted on the Pt-E surface at a fixed potential of −8 mV for a period of 800 s, along the lines of the protocol detailed above.

## Results and Discussion

### *Influence of Diffusion Pores*

A CV scan was initiated from OCP (283 mV) and swept negatively towards the cathodic region to +395 mV to initiate the reduction of Cu(II) and then in the opposite anodic direction to −260 mV to facilitate the oxidation of Cu(II) to Cu(I) as shown in Eq. 2 below:

$$Cu(NH_3)_4^{2+} + e^- \rightleftharpoons Cu(NH_3)_2^{+} + 2NH_3 \quad (2)$$

Following the studies on the oxidation-reduction profile, −8 mV was selected as the operating potential for all potentiostatic tests for the isolated generation of sufficient Cu(I) species in the system. With the model diffusion pores stacked onto the model cell to a desired length (denoted *l* mm) and the probe disk inserted within the stack at a desired position (denoted *y* mm), potentiostatic tests were initiated and the current density monitored over time, generating the current density profile shown in Fig. 3a.

The observed current responses in Fig. 3a show initially high cathodic current responses which are comparable to the current response observed in this region from the preliminary CV scans. Thereafter, a rapid decrease in the cathodic response was observed in the first 50 s, before a subsequent steady plateau after ca. 600 s. While preliminary experiments with longer time frames were conducted, the current response showed no subsequent decrease in the longer time frames. It can be inferred from the decrease in current response and the shape of the curve that there was a build-up of Cu(I) at the Pt-E surface that hindered the diffusion and resulting replenishment of Cu(II) at the electrode surface. Although the operating potential was selected within a region where mass transfer limitations were not significant during the relatively rapid CV scan, it would seem that the introduction of diffusion pores reintroduced diffusion limitations over time into the system. Operating at potentials lower than −8 mV would exacerbate this effect, as this would provide higher cathodic overpotentials for the reaction, hence faster kinetics. Although operating at higher potentials would result in slower kinetics, the build-up

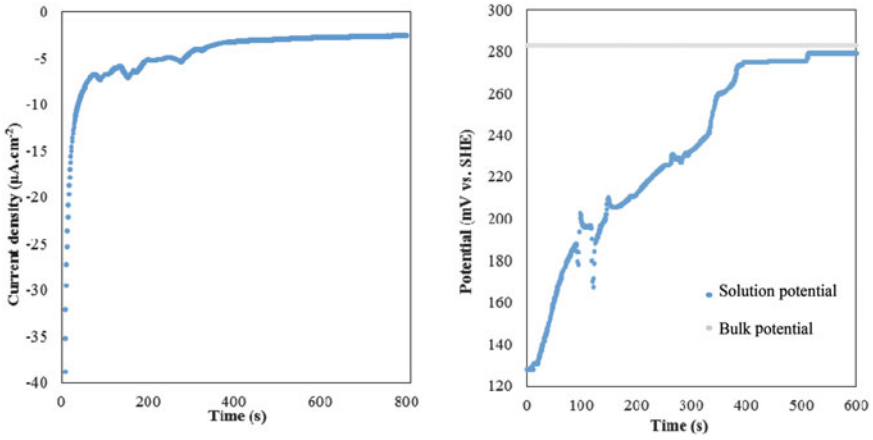


**Fig. 3** **a** Cathodic potentiostatic test, potential set at -8 mV versus SHE in a solution with base operating conditions, l = 10 mm, (Pt-E reaction surface area = 0.02356 $cm^2$). **b** Solution potential measured by a platinum probe placed at *y* = 0.25 mm from the reaction surface in an *l* = 10 mm diffusion pore, under base operating conditions. Measurement began immediately after terminating the cathodic reaction at the surface

of Cu(I) would still be observed if the potential at the surface is conducive to the cathodic reaction. Hence, regardless of the actual operating potential, a steady state is gradually achieved in which the rate of electrochemical reduction at the surface is balanced by the rate of migration of Cu(II) to, and Cu(I) away from the surface.

It was initially assumed that immediately after the termination of the potentiostatic test, the residual concentration variation, resulting from the surface reaction, would still be effective and detectable. For a period of ca. 10 s, the initial solution potential in Fig. 3b remained steady, thus confirming this assumption. The initially steady potential measurements suggest that readings within this period would be representative of a potential measurement taken whilst the steady state reaction occurred at the surface. As anticipated, over the subsequent 600 s the solution potential at $y = 0.25$ mm increased until it was within 10 mV of the initial solution potential. However, there was no clear trend in the rate of increase of the potential for repeat experiments conducted under the same conditions.

## *Potential Profiles Along Fixed Diffusion Pore Length*

The focus of this study were particles found in heap leaching operations where the average ore particle size is less than 25 mm [5]. Considering an ideal spherical particle with the value mineral at the centre, it can be assumed that the maximum straight pore length would be less than 12.5 mm across all directions. Therefore a fixed pore length ($l$) of 10 mm, with the probe position ($y$) being varied, was used in subsequent studies. A potential profile was generated by varying the probe position (y) along the fixed length is displayed in Fig. 4.

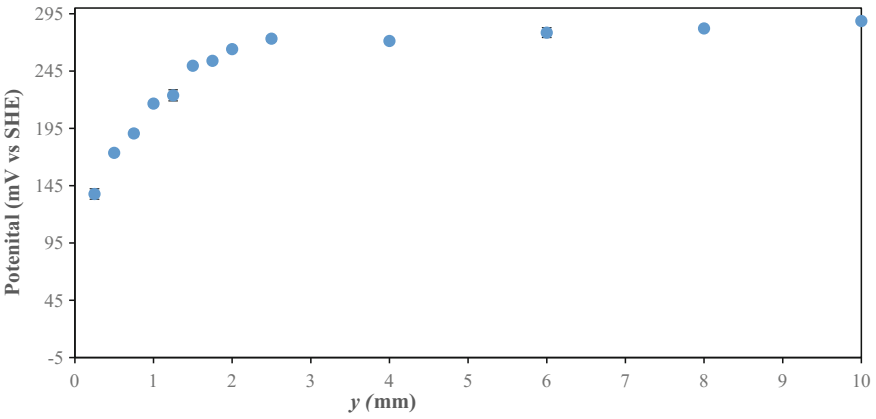


**Fig. 4** Potential profile along the fixed length ($l = 10$ mm) diffusion pore. Potential measurements were taken after immediate termination of the cathodic surface polarisation

For the 10 mm diffusion pore, there was a steep increase in solution potential in the first 2 mm and a subsequent plateau beyond as it reaches solution potential values close to the initial bulk solution. The measured potentials at $y > 2$ mm are between the fixed surface potential (−8 mV) and the bulk potential (283 mV); they are intermediates between the two values—a transitional region between the surface potential and the bulk potential. The presence of diffusion pathways results in a region ($y < 2$ mm) with significantly different solution properties.

As the experimental model in this study was an idealised mineral leach system, there were three competing factors that would result in the presence of this region (y > 2 mm):

- The rate at which Cu(II) was delivered to the electrode surface became potential determining and rate limiting with the introduction of diffusion pores.
- There was insufficient dissolved oxygen within the pores for reaction with the Cu(I), as the homogeneous reaction is known to be rapid.
- The rate at which Cu(I) was transported away from the reaction surface.

## *Potential Profiles Along Diffusion Pores of Varying Lengths*

It was observed there exists a region in the first 0.5 mm where the measured potential was independent of the pore length as shown in Fig. 5. This suggests that there are sub-processes that determine the solution potential closer to the surface, irrespective of the overall pore length and that these are related to the surface reduction reaction.

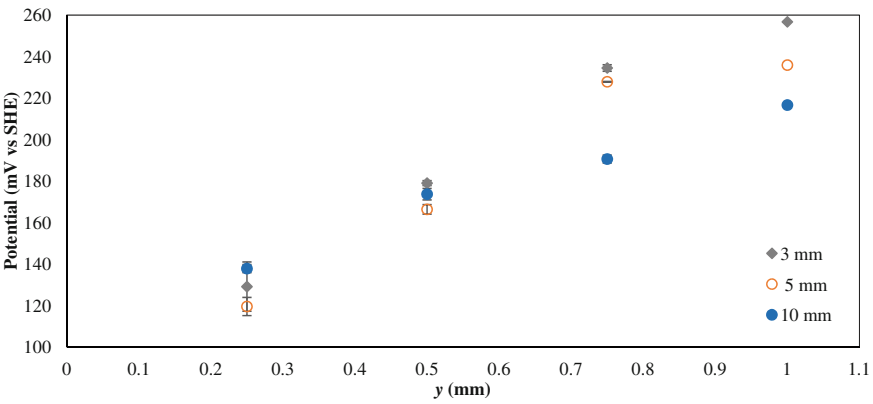


**Fig. 5** Potential profiles generated along varying diffusion pore lengths ($3 < l < 10$ mm, $0.25 < y < 1$ mm). Measurements taken after immediate conclusion of the cathodic polarization phase

## *Influence of Initial Cupric Ion Concentration*

Preliminary experiments were conducted within the concentration 0.13 < [Cu(II)] < 2.5 g/L to allow for a sufficiently broad range for analysis. Supplementary experiments conducted at [Cu(II)] < 0.5 g/L gave non-reproducible data. This was attributed to the decreased conductivity, hence higher solution resistance, caused by the lower concentrations of the electroactive [Cu(II)] species. Therefore experiments were conducted within 0.5 g/L< [Cu(II)] < 2.5 g/L, using three different concentrations which resulted in varied initial bulk solution potentials; 283 mV for 0.5 g/L, 292 mV for 1.3 g/L and 300 mV for 2.5 g/L. Figure 6 shows the current density response obtained from three initial Cu(II) concentrations at a fixed potential of −8 mV and a diffusion pore length of $l = 10$ mm.

The cathodic current response observed in Fig. 6a decreased proportionally with increasing initial concentration. This is indicative of a first order cathodic reaction with respect to [Cu(II)].

Figure 6b shows the potential profile generated when the initial [Cu(II)] was varied within the aforementioned [Cu(II)] range. The probe position, $y$, was limited to 4 mm, as it was noted that the effective diffusion region was within $y < 2$ mm. A similar trend of a rapid increase in the potential was observed in the first 2 mm thus confirming the presence of the active region

Increasing the initial [Cu(II)] from 0.5 g/L to 1.3 g/L resulted in a steeper concentration profile throughout the length of the pore. However, at a higher concentration of 2.5 g/L, the solution potential was consistently lower throughout the length of the pore. Moreover, there was a stagnation in the potential profile

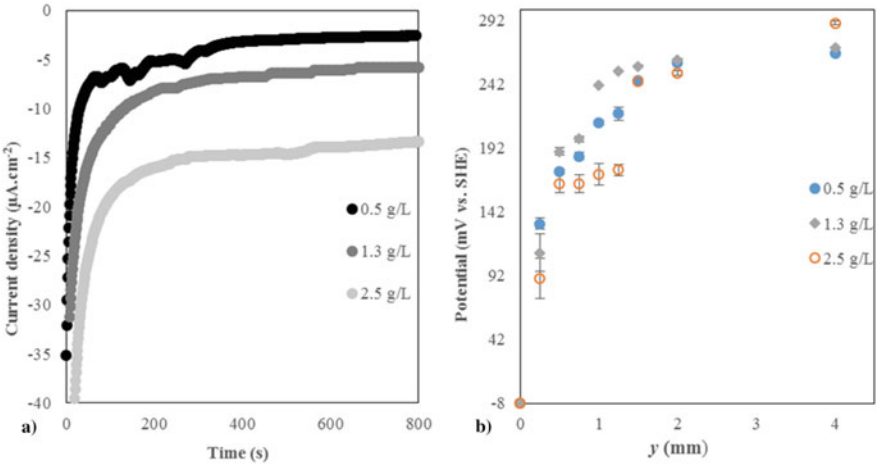


**Fig. 6** **a** Cathodic potentiostatic responses for varying initial cupric ion concentrations, potential set to −8 mV versus SHE, pore length set to l =10 mm. **b** Potential profile along the l = 10 mm diffusion pore at varying initial cupric ion concentration. Measurements were taken immediately after the termination of the polarization phase

between $0.5 < y < 1.25$ mm. These two features of the 2.5 g/L [Cu(II)] curve suggest a possible build-up of Cu(I) within the pore which hindered the replenishment of Cu(II) at the reaction surface. This suggests that at higher concentrations, due to higher rates of Cu(I) generation, either the transport or the re-oxidation of Cu(I) became potential determining.

## *Influence of Dissolved Oxygen*

As Cu(I) readily reacts with dissolved oxygen, there was difficulty in isolating the effect of transportation of Cu(I) away from the Pt-E surface from the re-oxidation reaction. Therefore the effect of oxygen was evaluated by testing the system in the presence of air, oxygen and under nitrogen. Since neither nitrogen nor oxygen are charged species, the addition of either gas did not have an effect on the current response at the surface and resulted in current density profiles similar to those obtained in Fig. 3a.

Evident from Fig. 7, higher concentrations of oxygen did not have a pronounced effect on the potential profile for $y < 0.5$ mm. The potential values at $y > 0.5$ mm for the nitrogen and air curves were numerically similar, which makes it unclear if the system was devoid of oxygen in both systems at $y > 0.5$ mm. Alternatively, the trace amounts of oxygen available in the nitrogen system were sufficient to support a re-oxidation rate that was comparable with that of the oxygen available in air.

A quantitative analysis using the current density graphs obtained in Fig. 3a over the length of the pore, using Simpson's Rule, showed that there was still just sufficient oxygen for the rapid re-oxidation reaction at $y = 0.5$ mm whereas the system was devoid of oxygen at $y < 0.5$ mm, used up by Cu(I) generated during the polarisation phase. The similarities in potential between the air, nitrogen and oxygen curve in Fig. 7. suggest that the system was somewhat devoid of oxygen for

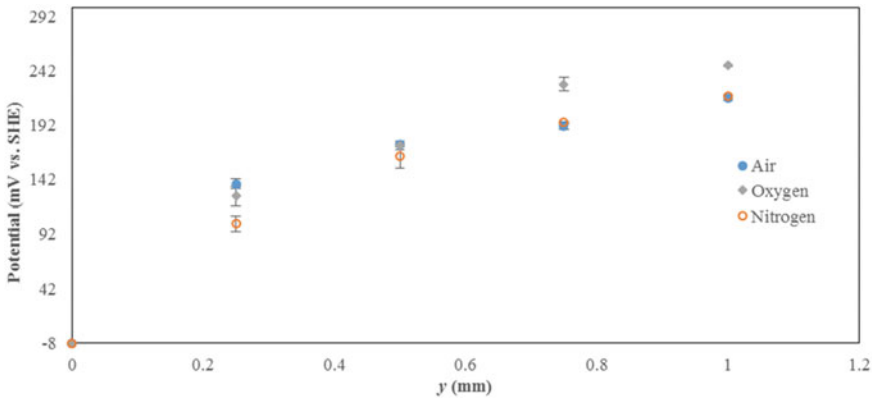


**Fig. 7** Potential profile along l = 10 mm diffusion pore in varying concentrations of oxygen

at least $y \leq 0.5$ mm. This further suggests that part of the dissolved oxygen contributed to the re-oxidation reaction but equilibrium and a consequent reaction zone at $y > 0.5$ mm in the presence of pure oxygen was rapidly established. The similarities between the air and the nitrogen curve in Fig. 7. suggest that the equilibrium and reaction zone was established at $1 < y < 2$ mm in the presence of oxygen.

## Conclusion

The length of the diffusion layer ($y < 0.5$ mm) across all potential profiles within the diffusion pores, irrespective of pore length, showed that the transport of Cu(I) away from the reaction surface had the most significant influence on the electrochemical profiles. This was further supported by the insignificant effect of varying concentrations of both Cu(II) and dissolved oxygen on the solution potential at $y < 0.5$ mm. The length of the diffusion layer ($y > 2$ mm) across all potential profiles for the 10 mm pore, alluded to the presence of a reaction zone located between $1 < y < 2$ mm within the 10 mm pore where Cu(I) must be transported, in order for the re-oxidation reaction to occur. Increasing the concentration of oxygen in the system did not have a marked influence on the potential closer to the surface, as experimental data showed that the system was devoid of oxygen at $y \leq 0.5$ mm. It can be inferred from Fig. 6b that there was an optimal initial [Cu(II)] between $1.3 <$ [Cu(II)] $< 2.5$ g/L where the effect of faster kinetics and higher [Cu(II)]/[Cu(I)] were balanced, thus resulting in the steepest potential profile. This optimal initial [Cu(II)] would be the ideal operating initial [Cu(II)] and would result in the lowest potential variations within the diffusion pores.

The hindered mass transport of dissolved species within diffusion pores results in a micro-environment within the pores, with significantly different solution properties from the bulk solution. The potential, at constant pH, of the system dictates the regions of thermodynamic stability. Therefore specific reactions are only thermodynamically feasible, and the products stable, within specific potential windows. As demonstrated in the present study, variations in the concertation of the redox couple within the pore resulted in the potential of the solution in the immediate vicinity of the mineral surface being significantly different from the potential of the bulk solution. In the absence of agitation, as is the case in heap leaching, the build-up of reduced species near the value mineral surface would cause a decrease in potential of solution in the immediate vicinity of the reaction surface. Consequently, the redox environment in the vicinity of the mineral surface could be inhibitive to leaching or possibly result in the formation of undesired but thermodynamically stable products, such as precipitates and deposits, in the system. Moreover, the leach kinetics of mineral dissolution by a redox reaction have been shown to be a strong function of the electrochemical potential at the mineral surface [9, 10].

The experimental model presented herein provided an experimental framework for representing and analysing the dissolution behaviour of mineral grain embedded within larger particles, such as those typically encountered in heap leaching. The model may be applied in dissolution studies of natural mineral, in order to identity the diffusion pathways of reactive species and the appropriate diffusion model to be used in the particle-scale modelling and optimization of the heap leaching process. The advancement of this work, in conjunction with more complex mass and heat transfer and reaction kinetics data, would allow for the modelling of particle-scale dissolution behaviour of natural minerals with varying porosities. A fully developed understanding of the complex particle-scale processes within the heap would allow for the optimization of the traditionally slow leaching process

**Acknowledgements** The authors wish to acknowledge support from the South Africa National Research Foundation (NRF) through the SARChI Chair in Minerals Beneficiation (Grant No 64829) and their Incentive Program for Rated Researchers (No 85864). The University of Cape Town is also acknowledged for support through their URC Block Grants.

## References

1. Padilla G, Cisternas L, Cueto J (2008) On the optimization of heap leaching. Miner Eng 21:673–683
2. Ghorbani Y (2012) On the progression of leaching from large particles in heaps. University of Cape Town (PhD Thesis), Cape Town
3. Malmstrom M, Berglund S (2008) Combined effects of spatially variable flow and mineralogy on the attenuation of acid mine drainage in groundwater. Appl Geochem 23(6):1419–1422
4. Liddell K (2005) Shrinking core models in hydrometallurgy: what students are not being told about the pseudo-steady state assumption. Hydrometallurgy 79(1–2):62–72
5. Ghorbani Y, Becker M, Mainza A, Franzidis J, Petersen J (2011) Large particle effects in chemical/biochemical heap leach processes-a review. Miner Eng 24(11):1172–1184
6. Petersen J, Dixon D (2006) Modelling and optimization of heap leach processes. In: Rawlings D, Johnson B (eds) Bioming. Springer, Berlin, pp 153–176
7. Meng X, Han K (1996) The principles and application of ammonia leaching of metals—a review. Miner Process Extr Metall Rev 16:23–61
8. Nicol M, Basson P (2017) The anodic behaviour of covellite in chloride solutions. Hydrometallurgy 172:60–68
9. Nicol M, Lazaro I (2002) The role of EH measurements in the interpretation of the kinetics and mechanisms of the oxidation and leaching of sulphide minerals. Hydrometallrgy 63: 15–22
10. Nicol M (1975) An electrochemical investigation of the dissolution of copper, nickel and copper-nickel alloys in ammonium carbonate solutions. J S Afr Inst Min,. 275–302